J|A|C|S COMMUNICATIONS

Published on Web 08/11/2009

Guest Tunable Structure and Spin Crossover Properties in a Nanoporous Coordination Framework Material

Suzanne M. Neville,[†,‡] Gregory J. Halder,[§] Karena W. Chapman,[||] Martin B. Duriska,[‡] Boujemaa Moubaraki,[‡] Keith S. Murray,[‡] and Cameron J. Kepert*[,†]

School of Chemistry, University of Sydney, NSW 2006, Australia, School of Chemistry, Monash University, VIC 3800, Australia, Materials Science Division, Argonne National Laboratory, Argonne, Illinois 60439, and X-ray Science Division, Advanced Photon Source, Argonne National Laboratory, Argonne, Illinois 60439

Received June 30, 2009; E-mail: c.kepert@chem.usyd.edu.au

The development of functional materials with physical properties that can be controlled on the molecular level is an important goal for the realization of nanoscale devices.[1,2] To this end, spin crossover (SCO) materials, which show dramatic switching responses (including with bistability) to external perturbations (e.g., temperature, pressure, magnetic field, light, and guest/chemical environment), have been actively investigated.[2−4] While the SCO phenomenon itself has been known for more than 70 years and extensive understandings of the process developed,[5] rational materials design in this area remains elusive due to the myriad solid state effects that influence SCO behavior. In an attempt to deconvolute these effects, extensive efforts have been devoted toward exploring the local influence of anion species, ligand functionality, and included guest molecules on SCO.[3,6−8] While some useful structure−property correlations have emerged, this approach has largely been frustrated by difficulties associated with preparing a broad series of analogous materials in which the crystal packing is not significantly altered.[6,9,10] The recent development of nanoporous spin crossover frameworks (SCOFs) provides a novel route to circumvent this problem, since the structural geometries of these materials are often only weakly perturbed by extra-framework species, which, in the case of neutral guests, may be conveniently exchanged *in situ* through desorption/sorption.[11−16]

In exploiting this approach, we have recently shown that guest size dramatically influences the SCO properties of a small-pore (*ca.* 4 Å) pillared-Hofmann material, $[Fe(pz)Ni(CN)_4]\cdot x$(guest) (pz = pyrazine), through a steric "internal pressure" mechanism in which host−guest attraction/repulsion between the pore walls strongly perturbs the crystal packing and therefore SCO energetics.[16] In an effort to explore the local electronic influence of sorbed guests, we turn our attention here to a much larger pore system, **SCOF-2(guest)**[15] (Figure 1; where **SCOF-2** is $[Fe(NCS)_2(bpbd)_2]$ and bpbd = 2,3-bis(4′-pyridyl)-2,3-butanediol), in which bulk steric influences are expected to have considerably less influence on the SCO properties due to the comparatively very loose packing of guests in the 1-D channels of this material.

Unlike its much more flexible isostructural SCOF analogues, in which substantial structural distortion accompanies guest exchange,[12] the **SCOF-2** structure is extremely rigid to guest removal and the SCO is retained.[15] As such, it is an ideal system through which to explore the local influence of guests on SCO. Following desorption then subsequent guest sorption, structural determinations were carried out for five guest-sorbed analogues of **SCOF-2(guest)**, where guest = acetonitrile (Acn), acetone (Ac),[15] methanol (Me), ethanol (Et), and 1-propanol (Pr), revealing the same tetragonal crystal symmetry (*P*4/*ncc*) and general framework connectivity (Figure 1).[17] Close examination of the structures revealed only very subtle variations in the iron(II) coordination environments (i.e., average Fe−N bond, N−Fe−N angle, etc.) and framework geometries (i.e., host−host interactions, grid dimensions, etc.). The most notable variation is in the interactions between the framework host and the guest species housed in its square 1-D channels (Figure 1b). In particular, while there are no significant host−guest interactions in the aprotic solvates **SCOF-2(Ac)** and **SCOF-2(Acn)**, host−guest hydrogen-bonding interactions (OH···S(CN)) are present in the protic solvates **SCOF-2(Me)**, **SCOF-2(Et)**, and **SCOF-2(Pr)** (see Supporting Information for full analysis).

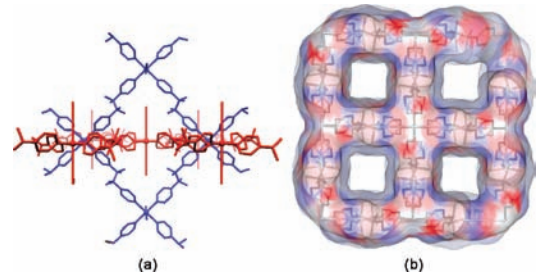

Figure 1. (a) Interpenetrating grid structure of **SCOF-2(guest)** and (b) square 1-D pores where guest molecules reside.

Despite the five different solvates having very similar structures, magnetic susceptibility measurements (275−15 K) revealed a range of SCO behaviors over this family, which include gradual, abrupt, and thermal hysteretic effects (Figure 2a and b). While each material undergoes a full one-step SCO, with the $\chi_M T$ values for each material at 275 and 15 K indicative of high spin (HS) and low spin (LS) iron(II) sites, respectively, the $T_{1/2}$ values span a *ca.* 50 K temperature range (Table 1). Also varying over this series is the abruptness of the SCO, such that the HS ↔ LS transition of the aprotic solvates occurs over wider temperature ranges than those of the protic guests. Of particular note is that the Me and Et solvates show significant thermal hysteresis of the $\chi_M T$ values over the heating and cooling modes, whereas the others do not.

The large variation in $T_{1/2}$ values across the series indicates that the guests significantly perturb the energetics associated with the SCO transition. This is likely through a combination of a change in ligand field energies at the iron(II) sites and modification of the lattice packing energies. With host−guest interactions expected to vary between the HS and LS states of the host due to the associated change in pore dimensions (Fe···Fe across the 1-D channels = *ca.* 14.6 Å (HS) and 14.3 Å (LS)), we note first that the general increase in $T_{1/2}$ values with increasing guest molecule size/volume

[†] University of Sydney.
[‡] Monash University.
[§] Materials Science Division, Argonne National Laboratory.
[||] X-ray Science Division, Argonne National Laboratory.

10.1021/ja905360g CCC: $40.75

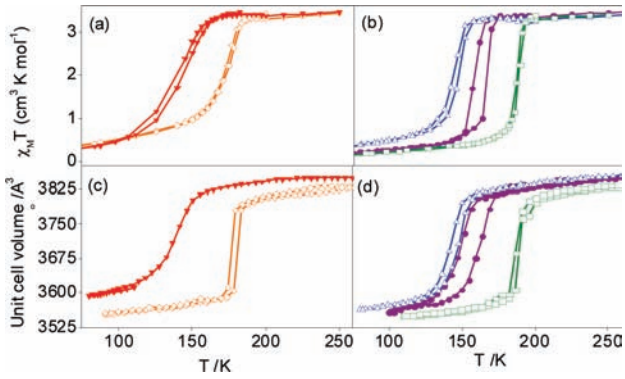

Figure 2. (a and b) $\chi_M T$ and (c and d) unit cell volume versus temperature for the aprotic (**SCOF-2(Acn)** (▼, red), **SCOF-2(Ac)** (◇, orange)) and the protic (**SCOF-2(Me)** (Δ, blue), **SCOF-2(Et)** (●, purple), **SCOF-2(Pr)** (□, green)) guests, respectively.

(Table 1) is the reverse of that expected from a simple "internal pressure" argument, in which bulkier guests are expected to favor the more open HS host lattice; the absence of a clear relationship here is perhaps unsurprising given that the guests are found to dock in different regions of the channels, with the smaller guests achieving a more optimal packing. It appears therefore that a more subtle guest-dependent effect is at play, involving both steric and electronic influences. In considering these inter-related influences on the iron(II) sites, we expect that guest variability would be reflected in intra- and intermolecular interactions; however, none of these parameters show any obvious correlation with the $T_{1/2}$ values (see Supporting Information). We thus turn our attention to the more subtle electronic influence of each guest molecule. In considering the local electric field associated with these, as quantified in the bulk by the dielectric constant, ε (which takes into account both the polarity and polarizability), we observe a general correlation between $T_{1/2}$ and ε for the guest molecules chosen; this is such that smaller ε values result in the LS state being stabilized (Table 1). Such a trend, which spans a large variation in ε, may indicate the presence of a second-coordination sphere effect in which the ligand field energies are influenced by framework polarization effects, either directly or through modification of the ligand charge densities.

In further structure-magneto studies on **SCOF-2(guest)**, the structural consequences over each spin transition were followed by variable temperature powder X-ray diffraction analysis using synchrotron radiation, a technique that allows very subtle changes in symmetry to be detected.[11,18,19] Data were collected upon continuous cooling from 260 to 90 K, then upon heating to 375 K to desolvate the framework, followed by cooling from 375 to 90 K, at 20 K h^{-1} under a helium atmosphere saturated with the desired solvent vapor. Thus, data were collected for each of the solvates upon cooling and subsequent heating through the SCO transitions. The qualitative structural behavior associated with SCO for each solvate is readily evident when the temperature dependence of the peak positions is compared, for example the {202} reflection, as illustrated in Figure 3. From this we see the continuous changes in lattice dimension associated with the variation in Fe−N distances as the SCO centers switch from HS→LS→HS states. It is also evident that the Me and Et solvates undergo a reduction in crystal symmetry *ca.* 40 K above their SCO transitions (as seen in the inequivalence of {202} and {022} at low temperatures; Figure 3). Upon Le Bail refinement[20] of the individual patterns for each solvate, the quantitative changes in unit cell volume versus temperature were compared and found to show excellent correlations with the SCO behavior derived from the magnetic data,

Table 1. Comparison of Magnetic and Structural Parameters[19,21]

guest	$T_{1/2}$ (↓/↑)/K	transition	guest size/Å^3	dielectric constant
Acn	137	no	45.9	37.5
Me	145/142	yes	34.1	32.6
Ac	162	no	64.5	20.7
Et	166/156	yes	49.8	24.3
Pr	187	no	65.7	20.1

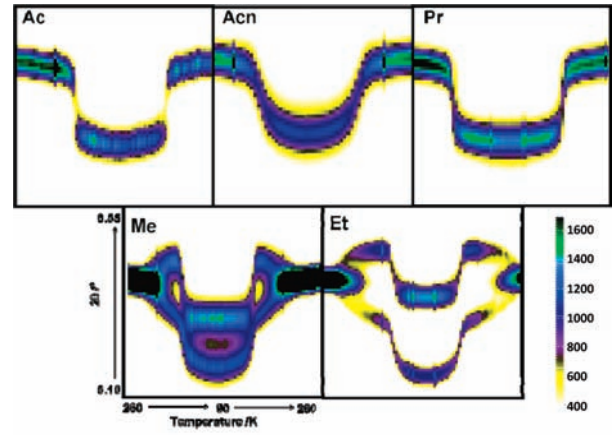

Figure 3. Powder diffraction peak evolution (6.10°−6.55°, {202} reflection) versus temperature (260−90−260 K).

including that of thermal hysteresis for the Me and Et solvates (see Figure 2c and d).

For the tetragonal Acn, Ac and Pr solvates, detailed examination of the peaks within selected patterns before (HS), during (HS/LS), and after (LS) the spin transitions reveals two structural behaviors (Figures 3 and 4). For **SCOF-2(Acn)**, which shows the most gradual spin transition from magnetic susceptibility measurements, a continuous shift in Bragg reflections from tetragonal HS to LS states was observed. This closely matches the magnetic data, indicating that the broadness of the transition is intrinsic to the material and arises with the continuous SCO of iron(II) sites within individual crystallites, rather than being caused by sample broadening associated with crystallite heterogeneity (which would lead to peak broadening or splitting). For **SCOF-2(Ac)** and **SCOF-2(Pr)**, two-phase regions exist at intermediate spin transition temperatures where both HS and LS crystallites coexist; this appears to result from a small degree of sample broadening at an abrupt, although continuous, spin transition. Overall, the three solvates **SCOF-2(Acn)**, **SCOF-2(Ac)**, and **SCOF-2(Pr)** undergo gradual structural transitions that are conventionally associated with a moderate degree of lattice cooperativity and communication between SCO centers; this is consistent with structural findings on other systems that display gradual spin transitions.[10,14,22,23]

In contrast to the Acn, Ac, and Pr solvates, **SCOF-2(Me)** and **SCOF-2(Et)** both show very abrupt spin transitions with thermal hysteresis, indicative of a higher degree of lattice cooperativity.[22] Again, the SCO transitions are continuous, with there being no evidence for broadening associated with crystallite heterogeneity, as might arise with different degrees of guest sorption. Most notable is a transition to orthorhombic symmetry above the SCO transition for each of the phases. Indexing and inspection of the systematic absences of the orthorhombic phase both below and just above the SCO transition suggest the space group *Pccn*, corresponding to a halving in crystal symmetry with the retention of a single iron(II) site. This contrasts with the transition observed in the related material **SCOF-4(Ac)** ($P42_1c$ to $P2_12_12$), which similarly occurs prior to and independently of the SCO transition, leading to the

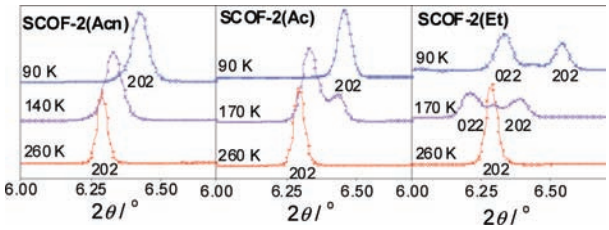

Figure 4. Powder diffraction patterns in HS, HS/LS, and LS states.

formation of alternating iron(II) sites.[11] Here, the retention of *c*-glide planes along *a* and *b* dictates that no such inequivalence arises, with the iron(II) site retaining 4-fold multiplicity above and below the transition. This observation is supported by the retention of a single-step SCO behavior. Single crystal analyses on **SCOF-2(Me)** and **SCOF-2(Et)** at 100(2) K failed initially to detect the symmetry change due to merohedral twinning of the orthorhombic phase and satisfactory refinement in *P*4/*ncc*. Upon subsequent structural refinement in *Pccn*,[24] a subtle ordering of the guest molecules was detected, with an associated distortion of the channels from square to rhombic geometry, likely driven by the side-by-side packing of these smaller guests within the wider regions of the channels.

The observance of hysteresis in framework materials that contain only flexible pyridyl linking ligands is highly unusual and suggests there is a degree of cooperativity within the lattice, an effect more conventionally associated with short rigid bridging ligands.[4,7] It is known that intermolecular lattice interactions, such as the guest−framework hydrogen bonding evident in the protic guest systems, can enhance the propagation of SCO in the solid state.[6] The more abrupt transitions seen for the protic solvates over those of the aprotic solvates likely result directly from this effect. The thermal hystereses seen in the Me and Et solvates are likely also to be attributable to some extent to such interactions, although the absence of any observed SCO hysteresis in **SCOF-2(Pr)**, despite the fact that this shows the most abrupt transition of the series, suggests that it is primarily the lower symmetry packing of the Me and Et solvates that is responsible for imparting hysteretic behavior to the SCO transition.

In summary, we have demonstrated that nanoporous framework materials can provide an ideal stage to examine the relative consequences of systematic structural perturbation on SCO. Explicitly, expansion of this SCOF phase to a large range of solvates has resulted in one of the first examples of rationally tunable guest-dependent behavior in an SCO system, whereby both the transition temperature and, perhaps most interestingly, the degree of lattice cooperativity can be manipulated by exchange of the guest molecule—a long sought-after goal in SCO research. Further guest variation in this system and in other SCOFs in the future will be important to gauge whether the steric and electronic correlations delineated can be applied globally. Moreover, this work and other recent studies which have been directed toward controlling SCO properties by alternate approaches, such as particle size reduction via nanoparticle growth,[2,25] provide a pivotal step toward manipulating magnetic properties on the molecular scale, which is a core goal for the eventual utilization of such materials in active devices.

Acknowledgment. This work was supported by an Australian Research Council Discovery Project Grant (DP0557000) and the Australian Synchrotron Research Program.

Supporting Information Available: Synthesis; crystallographic, magnetic, and thermogravimetric data. This material is available free of charge via the Internet at http://pubs.acs.org.

References

(1) Ozin, G. A.; Arsenault, A. C. *Nanochemistry: A Chemical Approach to Nanomaterials*; The Royal Society of Chemistry: Cambridge, 2005. Lin, W.; Rieter, W. J.; Taylor, K. M. L. *Angew. Chem., Int. Ed.* **2009**, *48*, 650–658. Kahn, O.; Larionova, J.; Yakhmi, J. V. *Chem.—Eur. J.* **1999**, *5*, 3343–3349.
(2) Létard, J.-F.; Guionneau, P.; Goux-Capes, L. *Top. Curr. Chem.* **2004**, *235*, 221–249.
(3) Gütlich, P.; Goodwin, H. A. *Top. Curr. Chem.* **2004**, *233*, 1–47.
(4) Kahn, O.; Martinez, C. J. *Science* **1998**, *279*, 44.
(5) Kahn, O. *Molecular Magnetism*; VCH: New York, 1993. *Spin Crossover in Transition Metal Compounds I*; Gütlich, P., Goodwin, H. A., Eds.; Springer-Verlag: Berlin, 2004; Vol. 233.
(6) Guionneau, P.; Marchivie, M.; Bravic, G.; Létard, J.-F.; Chasseau, D. C. *Top. Curr. Chem.* **2004**, *234*, 97–128.
(7) Garcia, Y.; Niel, V.; Muñoz, M. C.; Real, J. A. In *Spin Crossover in Transition Metal Compounds I*; Gütlich, P., Goodwin, H. A., Eds.; Springer-Verlag: Berlin, 2004; Vol. 233, pp 229−257.
(8) Leita, B. A.; Neville, S. M.; Halder, G. J.; Moubaraki, B.; Kepert, C. J.; Létard, J.-F.; Murray, K. S. *Inorg. Chem.* **2007**, *46*, 8784–8795.
(9) Ichiyanagi, K.; Hebert, J.; Toupet, L.; Cailleau, H.; Guionneau, P.; Létard, J.-F.; Collet, E. *Phys. Rev. B* **2006**, *73*, 060408−060401.
(10) Onishi, S.; Sugano, S. *J. Phys. C: Solid State Phys.* **1981**, *14*, 39–55.
(11) Halder, G. J.; Chapman, K. W.; Neville, S. M.; Moubaraki, B.; Murray, K. S.; Létard, J.-F.; Kepert, C. J. *J. Am. Chem. Soc.* **2008**, *130*, 17552–17562.
(12) Halder, G. J.; Kepert, C. J.; Moubaraki, B.; Murray, K. S.; Cashion, J. D. *Science* **2002**, *298*, 1762–1765.
(13) Murray, K. S.; Kepert, C. J. *Top. Curr. Chem.* **2004**, *233*, 195–228.
(14) Neville, S. M.; Halder, G. J.; Chapman, K. W.; Duriska, M. B.; Southon, P. D.; Cashion, J. D.; Létard, J.-F.; Moubaraki, B.; Murray, K. S.; Kepert, C. J. *J. Am. Chem. Soc.* **2008**, *130*, 2869–2876.
(15) Neville, S. M.; Moubaraki, B.; Murray, K. S.; Kepert, C. J. *Angew. Chem., Int. Ed.* **2007**, *46*, 2059–2062.
(16) Southon, P. D.; Liu, L.; Fellows, E. A.; Price, D. J.; Halder, G. J.; Chapman, K. W.; Moubaraki, B.; Murray, K. S.; Létard, J.-F.; Kepert, C. J. *J. Am. Chem. Soc.* **2009**, *131*, 10998–11009.
(17) Crystal data **SCOF-2(guest)^{as}** (HS state): **SCOF-2(Me)**: $Fe_2(NCS)_4(C_{14}H_{16}N_2O_2)_2\cdot 3(CH_4O)$, $M_r = 756.67$, orange rod, tetragonal, *P*4/*ncc*, $a = 14.675(3)$ Å, $c = 17.984(7)$ Å, $V = 3873.1(18)$ Å^3, $T = 200$ K, $Z = 4$, $r_{calc} = 1.277$ g cm^{-3}, μ(Mo K$_\alpha$) = 0. 547 mm^{-1}, GOF = 1.109, R_1 for $I > 2\sigma(I)$: 0.0790, wR_2 for all data: 0.3054. **SCOF-2(Et)**: $Fe_2(NCS)_4(C_{14}H_{16}N_2O_2)_2\cdot 3(C_2H_6O)$, $M_r = 798.72$, orange rod, tetragonal, *P*4/*ncc*, $a = 14.639(5)$ Å, $c = 17.851(12)$ Å, $V = 3825(3)$ Å^3, $T = 200$ K, $Z = 4$, $r_{calc} = 1.355$ g cm^{-3}, μ(Mo K$_\alpha$) = 0.558 mm^{-1}, GOF = 1.133, R_1 for $I > 2\sigma(I)$: 0.0880, wR_2 for all data: 0.3644. **SCOF-2(Pr)**: $Fe_2(NCS)_4(C_{14}H_{16}N_2O_2)_2\cdot(C_3H_6O)$ $M_r = 720.68$, orange rod, tetragonal, *P*4/*ncc*, $a = 14.7260(10)$ Å, $c = 17.899(3)$ Å, $V = 3881.5(7)$ Å^3, $T = 220$ K, $Z = 4$, $r_{calc} = 1.219$ g cm^{-3}, μ(Mo K$_\alpha$) = 0.539 mm^{-1}, GOF = 1.138, R_1 for $I > 2\sigma(I)$: 0.0807, wR_2 for all data: 0.3396. **SCOF-2(Acn)**: $Fe_2(NCS)_4(C_{14}H_{16}N_2O_2)_2\cdot 2(C_2H_3N)$, $M_r = 742.69$, orange rod, tetragonal, *P*4/*ncc*, $a = 14.6829(10)$ Å, $c = 17.920(3)$ Å, $V = 3863.2(7)$ Å^3, $T = 200$ K, $Z = 4$, $r_{calc} = 1.267$ g cm^{-3}, μ(Mo K$_\alpha$) = 0.544 mm^{-1}, GOF = 1.092, R_1 for $I > 2\sigma(I)$: 0.0779, wR_2 for all data: 0.3215.
(18) Bartel, M.; Absmeier, A.; Jameson, G. N.; Werner, F.; Kato, K.; Takata, M.; Boca, R.; Hasegawa, M.; Mereiter, K.; Caneschi, A.; Linert, W. *Inorg. Chem.* **2007**, *46*, 4220–4229. Neville, S. M.; Leita, B. A.; Offermann, D. A.; Duriska, M. B.; Moubaraki, B.; Chapman, K. W.; Halder, G. J.; Murray, K. S. *Eur. J. Inorg. Chem.* **2007**, 1073–1085.
(19) Hostettler, M.; Tornroos, K. W.; Chernyshov, D.; Vangdal, B.; Bürgi, H.-B. *Angew. Chem., Int. Ed.* **2004**, *43*, 4589–4594.
(20) Larson, A. C.; Von Dreele, R. B. Los Alamos National Laboratory Report, LAUR 86-748, 2000.
(21) Webster, C. E.; Drago, R. S.; Zerner, M. C. *J. Am. Chem. Soc.* **1998**, *120*, 5509–5516. Lide, D. R. *CRC Handbook of Chemistry and Physics*, 85th ed.; CRC Press: 2004.
(22) König, E.; Ritter, G.; Kulshreshtha, S. K.; Waigel, J.; Goodwin, H. A. *Inorg. Chem.* **1984**, *23*, 1896–1902.
(23) Sorai, M.; Seki, S. *J. Phys. Chem. Solids* **1974**, *35*, 555–570.
(24) Crystal data **SCOF-2(guest)^{rs}** (LS state): **SCOF-2(Me)**: $Fe(NCS)_2(C_{14}H_{16}N_2O_2)_2\cdot 3(C_3H_6O)$, $M_r = 756.68$, purple rod, orthorhombic, *Pccn*, $a = 14.3578(6)$ Å, $b = 14.3904(5)$ Å, $c = 17.8813(7)$ Å, $V = 3694.5(2)$ Å^3, $Z = 4$, $r_{calc} = 1.339$ g cm^{-3}, μ(Mo K$_\alpha$) = 0.574 mm^{-1}, GOF = 1.051, R_1 for $I > 2\sigma(I)$: 0.0631, wR_2 for all data: 0.1988. **SCOF-2(Et)**: $Fe(NCS)_2(C_{14}H_{16}N_2O_2)_2\cdot 3(C_3H_6O)$ $M_r = 798.74$, purple rod, orthorhombic, *Pccn*, $a = 14.4934(6)$ Å, $b = 14.5117(5)$ Å, $c = 17.8874(6)$ Å, $V = 3762.1(2)$ Å^3, $Z = 4$, $r_{calc} = 1.378$ g cm^{-3}, μ(Mo K$_\alpha$) = 0.567 mm^{-1}, GOF = 1.104, R_1 for $I > 2\sigma(I)$: 0.1088, wR_2 for all data: 0.2260.
(25) Molnár, G.; Cobo, S.; Real, J. A.; Carcenac, F.; Daran, E.; Vieu, C.; Bousseksou, A. *Adv. Mater.* **2007**, *19*, 2163–2167.

JA905360G